Observed Oceanic Variability at and near the Air-Sea Interface during Phase III of Project BOMEX

CLIFFORD A. JACOBS

The Center for the Environment and Man, Inc., Hartford, Conn. 06120

(Manuscript received 3 January 1977, in final form 14 June 1977)

ABSTRACT

The natural variability observed at and near the air-sea interface during Period III of Project BOMEX is examined. The time and space variability in the observed oceanic parameters is large by classical oceanographic standards. Several interesting features were found in this BOMEX data set. Changes in the 10 m wind speed appear to be correlated to the movements of shallow temperature and salinity fronts. A secondary maximum in the mean diurnal sea surface temperature variation consistently appears in the early morning (local time). The diurnal heating patterns in the mixed layer imply a relationship between the vertical density gradient and the intensity of the vertical turbulent mixing. This relationship is further explored in numerical model studies in a companion paper (Jacobs, 1978).

1. Introduction

The Barbados Oceanographic and Meteorological Experiment (BOMEX) took place in the summer of 1969 in an area east of the Lesser Antilles Arc. Fixed ship stations in an array, shown in Fig. 1, collected data on a 500 km × 500 km grid square. The principal objective of this experiment was to measure the rate of exchange of the properties—heat, water substance and momentum—between and within the tropical ocean and the overlying atmosphere.

The oceanic observational program has been described in detail elsewhere [see, e.g., Delnore and McHugh (1972) and BOMEX field observations and basic data inventory, BOMAP (1971)]. The atmospheric and oceanographic data collected during BOMEX have been used in a number of studies of the natural variability of the marine tropical environment (cf. Landis, 1971; Pond *et al.*, 1971; Holland, 1972; Delnore, 1972; Pandolfo and Jacobs, 1972). During the preparation of Period III oceanographic and atmospheric observations for a numerical model study described in Jacobs (1976), some previously unreported events in the oceanic mixed layer were revealed. Also, the natural variability in the mixed layer on a diurnal scale was examined in detail. This paper reports the results of that examination.

2. A general description of the observations

During Period III, five ships occupied the approximate positions shown in Fig. 1. At these positions a number of oceanic observations were made starting at most ships at 0000 GMT 21 June and continuing until about midday on 2 July. A maintenance and calibration day was set aside on 27 June and few, if any, observations are reported at that time. Thus, the Period III oceanic data set consists of 10 days of data collected over an 11-day period. Examined in this study are the observed wind speed (from the boom at 10 m above the sea surface), water temperature (at the surface from bucket thermometer and boom thermistor records and below the surface from STD soundings) and salinity (below the surface from STD soundings). The examination of these data was carried out at the three ships *Discoverer*, *Oceanographer* and *Mt. Mitchell*. The omission of reported analyses for the other two ships is explained in Jacobs (1976). More detailed information about the observations and their preparation is also presented there. This paper presents a general discussion of several aspects of the Period III data set.

The boom observations of the wind speed consist of 10 min averages over an 11-day period (approximately 1100 observations per ship). A nearly steady easterly wind direction was reported at the three ships during this period.

STD soundings were made eight times a day at the *Discoverer* and *Oceanographer* and four times a day at the *Mt. Mitchell*. At the sea surface, bucket observations were taken every 2 h and continuous 10 min average boom temperatures were recorded.

The boom and bucket temperatures are generally in good agreement, but there are some discrepancies. There are several possible reasons for these

0022-3670/78/0103-0118$08.00

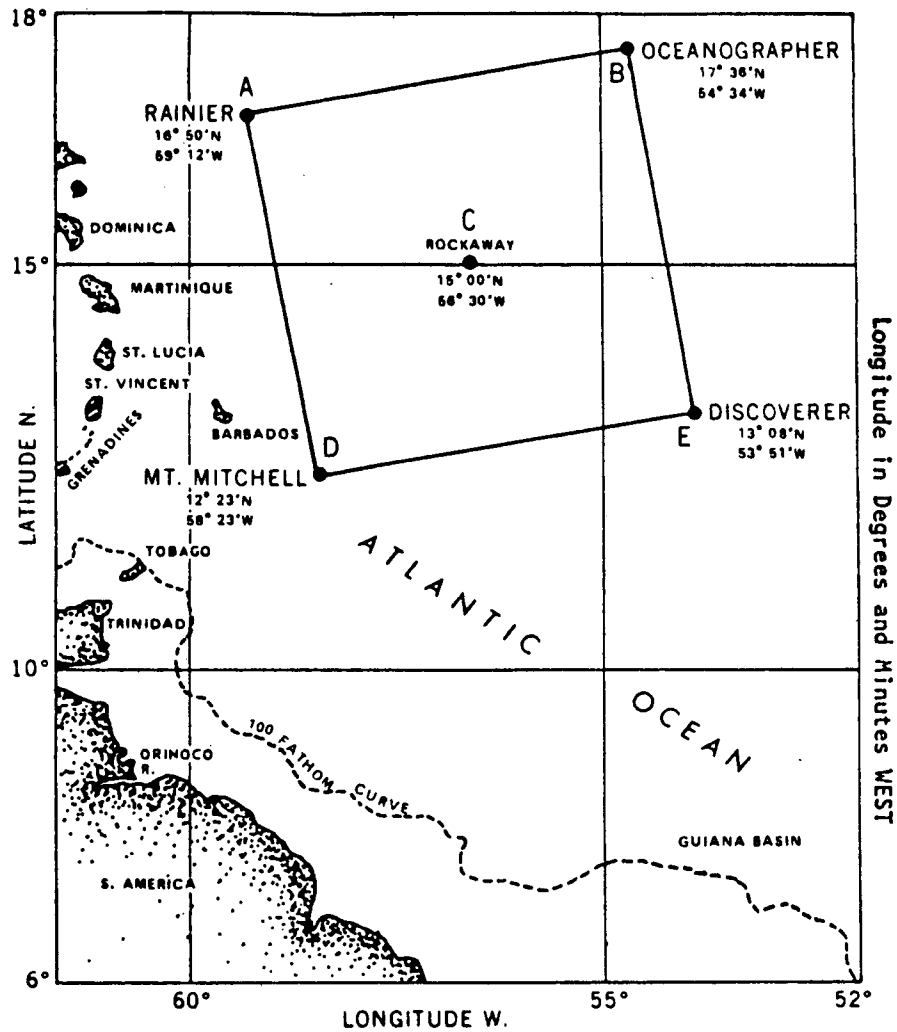

FIG. 1. Position of fixed ship stations during Period III of BOMEX (from Delnore, 1972).

differences. First, there are inaccuracies in calibration and incorrect or improperly recorded data values (both of which appear to occur). Next, there is the difference in recording precision of the two instruments. The bucket temperature is reported to the nearest tenth of a degree (°C) and the boom temperature is recorded to the nearest thousandth of a degree (°C). It is also likely that the bucket method of measuring the temperatures senses a different environment than the boom method. The bucket sampler is large enough to disturb any near-surface vertical temperature gradients[1], and therefore to provide a water sample which is a mixture over a layer 50–100 cm deep. The boom sensor is a small thermistor which is suspended at a constant distance (~20 cm) below the undulating sea surface. Further complicating the issue is the instrument location with respect to the ship. Bucket samples are generally taken over the side which allows for the possibility of contamination of the observation by ship outflows (i.e., engine cooling water and sewage). The boom sensor was located several meters off the bow which placed it further away from possible contaminating sources.

One of the results of the analyses is diurnal temperature fluctuation presented in terms of the average temperature departure (for a given hour of the day) from the 5-day average temperature at a given level. This means that the diurnal temperature variation is resolved with eight values a day for the *Discoverer* and *Oceanographer* and four values a day for the *Mt. Mitchell*. Two curves of the

[1] Strong temperature gradients in the top millimeter of the ocean have been described by MacIntyre (1974). It is also likely that under certain atmospheric conditions, particularly at night, temperature gradients near the surface (down to ~10 to 100 cm) can develop. There is some indication of this even in the mean diurnal temperature variation at the surface at each of the three ships.

mean diurnal variation in the sea surface temperature are constructed—one for the boom temperatures and the other for the bucket temperatures. However, the sea surface temperature observations are taken more frequently, permitting temperature departures at 2 h intervals to be calculated. The temperature departures are presented at the surface and at six subsurface levels down to a depth slightly below the depth of penetration of the diurnal temperature departures.

Finally, it should be noted that the ships were unable to maintain their deep sea moorings during Period III, and were forced to operate in a steam-and-drift mode to remain near their stations. Therefore, time series presentation of the water temperatures and salinities at any of the ships must be interpreted carefully in order to determine if the variations are due to changes in ship location in the presence of horizontal gradients. At each ship, there are a few short periods (of ~1-day duration) in which one location was maintained. These brief intervals are indicated on the time series plots of water temperatures and salinities for the respective ships which follow.

a. Observations at the Discoverer

Most of the STD observations at the *Discoverer* were taken within a circular area of about 22 km centered about the mean ship position. Three stations designated U, V and W were maintained

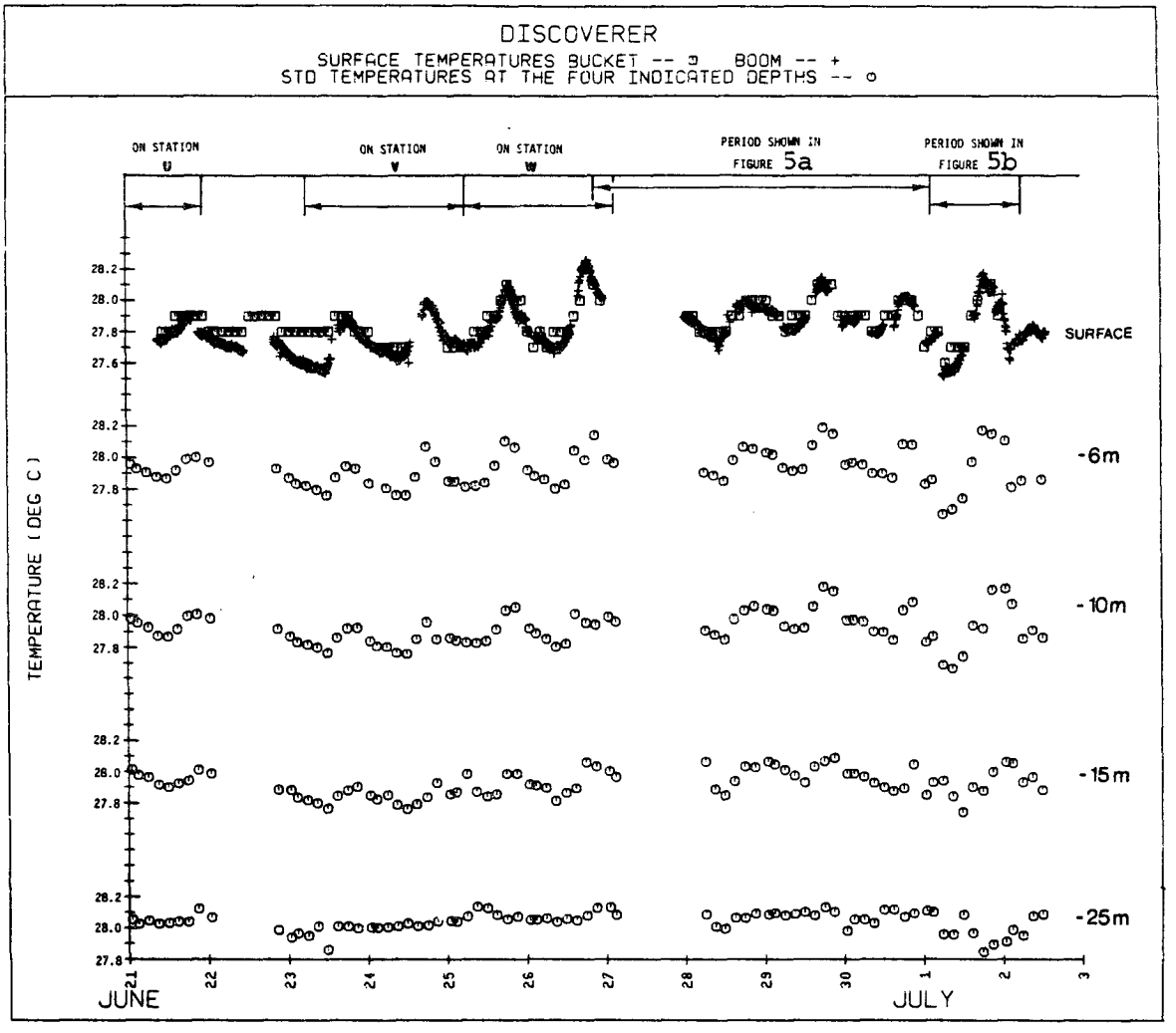

FIG. 2. Water temperatures at *Discoverer* at sea surface and four subsurface depths are shown as a function of time during Period III. Temperature measurements were made by bucket and boom sensors at surface and by STD soundings at subsurface levels (see box above the figure for symbol designation). At top of temperature axis, the periods for which the ship was on-station are indicated. The two periods shown at top of the temperature axis indicate when salinity data at −6 m are presented in Fig. 5.

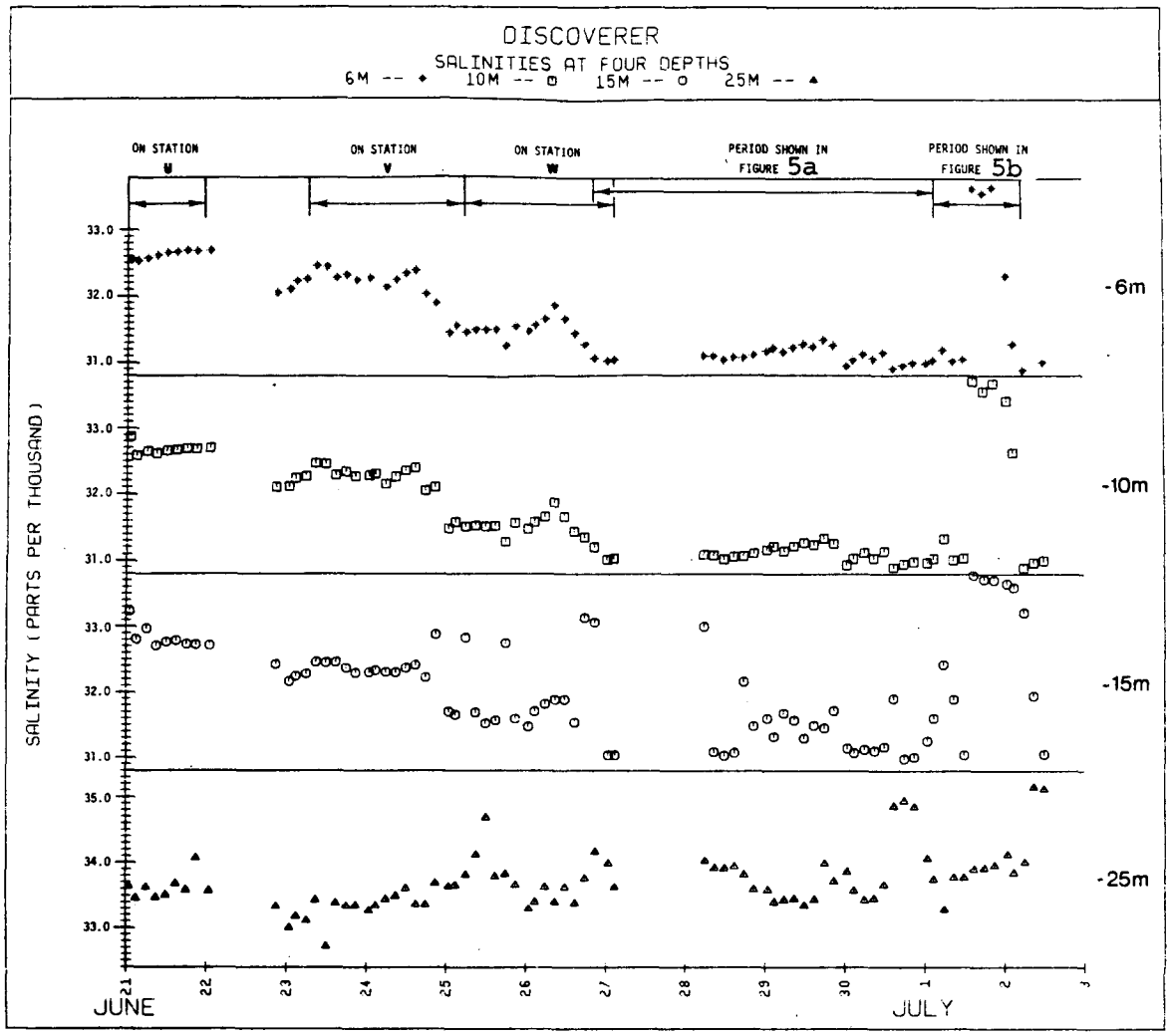

FIG. 3. Salinity at *Discoverer* at four subsurface depths, as a function of time during Period III (see box above figure for symbol designation). At top of salinity axis, the periods for which the ship was on-station are indicated. The two periods shown at top of salinity axis indicate when salinity data at −6 m are presented in Fig. 5.

for about a day or more during Period III [Delnore and McHugh (1972); also see Figs. 2, 3, and 5].

The sea surface temperatures (measured by bucket samples and from a boom) and the subsurface temperatures (measured by STD soundings at four depths of −6, −10, −15 and −25 m) are presented for a 12-day period at the *Discoverer* in Fig. 2. The salinities at the four subsurface depths and for the same period are given in Fig. 3. (The periods during which the ship was able to maintain a fixed position are indicated on the top of each of these figures.)

In the time series for all three ships, at least one rapid change in temperature and/or salinity is apparent in the mixed layer (see Figs. 2, 3, 8, 9, 13 and 14). Large spatial variability in salinity due to isolated "lenses" of low-salinity water is not uncommon in this region of the ocean (Ryther *et al.*, 1967; Metcalf, 1968). Landis (1971) and others have attributed these low-salinity lenses to Amazon River water, but a careful study of the local rainfall, oceanographic conditions and the Amazon River outflow led Neumann (1969) to conclude that a close inverse correlation between local rainfall and surface salinity is indicated.

There is some evidence to suggest that these rapid changes in salinity and/or temperature are correlation to the onset of trends in the 10 m wind speed (Figs. 4, 10 and 15). This correlation suggests a possible relationship between the movements of low-salinity lenses and the near-surface wind.

During the second part of this 12-day period (28 June to 3 July) the *Discoverer* occupied many widely spaced stations. During this period, there was apparent a strong haline front with an

associated weak thermal front in the area through which the ship was moving. As a consequence, explanation of trends in recorded temperature and salinity during this period becomes difficult. However, salinity maps at −6 m may be drawn for two periods during the second half of the 12 observation days. The implicit assumption underlying the construction of these maps is that the conditions in the surface layers of the ocean are quasi-static during the periods displayed, and that a realistic picture of the horizontal distribution of the salinity can therefore be obtained.

The first period presented is from 2100 GMT 26 June to 0100 GMT 1 July. An inferred salinity map for this period is shown in Fig. 5a. Since the ship was drifting during the first period, it can be seen from Figs. 3 and 5a that there is little horizontal variation of the salinity within the upper 10 m. A second set of salinities is mapped for a 24 h period beginning at 0300 GMT 1 July and is shown in Fig. 5b. The beginning of the second period (which coincides with the end of the first period) is chosen to correspond to two events: 1) the return of the *Discoverer* to its mean position from an extreme departure (13°05′N and 53°11′W, not shown in Fig. 5); and 2) the onset of a brief decline in the wind speed (see Fig. 4).

In Fig. 5b, a salinity "front" which appeared in the area on 1 July is clearly apparent. This front is seen in the salinity time series (Fig. 3) as a vertically coherent salinity "spike" which is visible down to −15 m. The time and value of the individual observations presented in Figs. 5a and 5b are given next to each observing location so that the horizontal salinity distributions may be synchronized with the temporal salinity display (Fig. 3). It should be noted that not all of the points which appear on the map (Fig. 5b) are shown in the salinity time series (Fig. 3). In Fig. 3, only the data obtained at the eight regularly scheduled observation times are presented.

The observation which marks the passage of the *Discoverer* through the front was taken at 13°07′N, 53°38′W at 1500 GMT 1 July. The ship occupied the same position 14 h later (0600 GMT 2 July), and recorded the lowest salinities, at −6 and −10 m, of the entire 12-day period. This observation is shown in Fig. 3 as the first point after the end of the second period mapped. However, the same observation indicates that the front is still present at −15 m. Furthermore, the disappearance of the higher salinity water in the surface layer early in the day on 2 July also corresponds to periods of rapidly increasing wind speed (see Fig. 4).

The weak thermal "cool" front that precedes the salinity front by several hours (Fig. 3) results in the coldest temperature at each level for the 12-day period. These temperature minima do not occur at the same time at all depths, but occur (in the vertical) at successively later times with increasing depth. Furthermore, the lowest temperature minimum occurs at the surface with the subsurface minimum temperature increasing with increasing depth. Maps of the temperature for the two periods for which the salinity was presented are not shown because the diurnal range of temperatures equals or exceeds the range of any transient temperature changes.

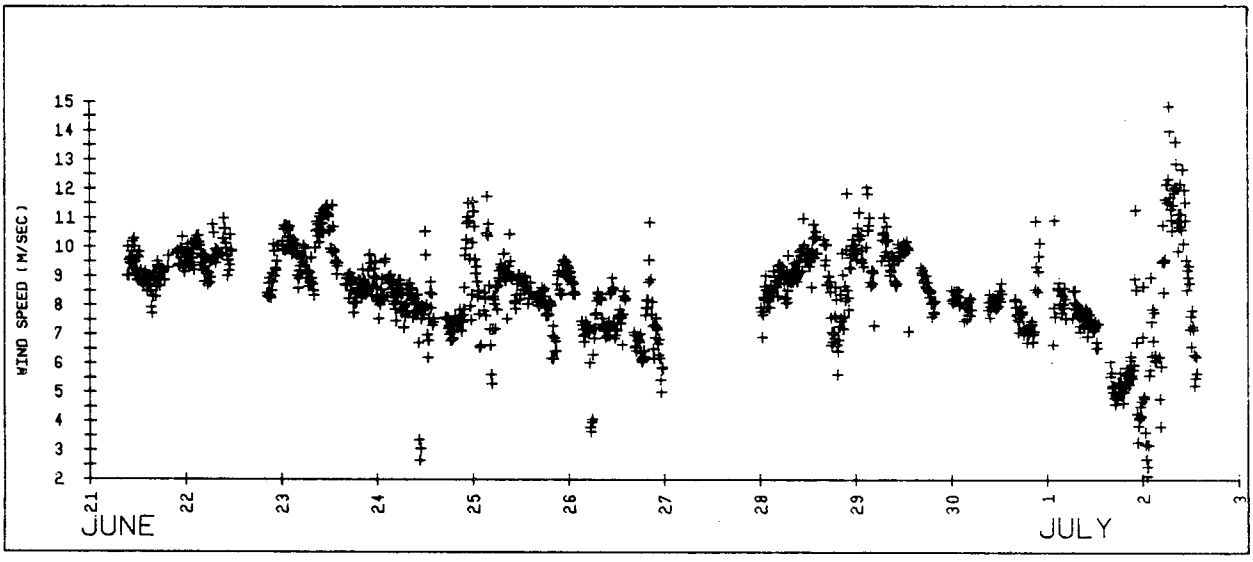

FIG. 4. *Discoverer* boom observations of wind speed at 10 m above sea surface during Period III. Each point represents a 10 min average of wind speed.

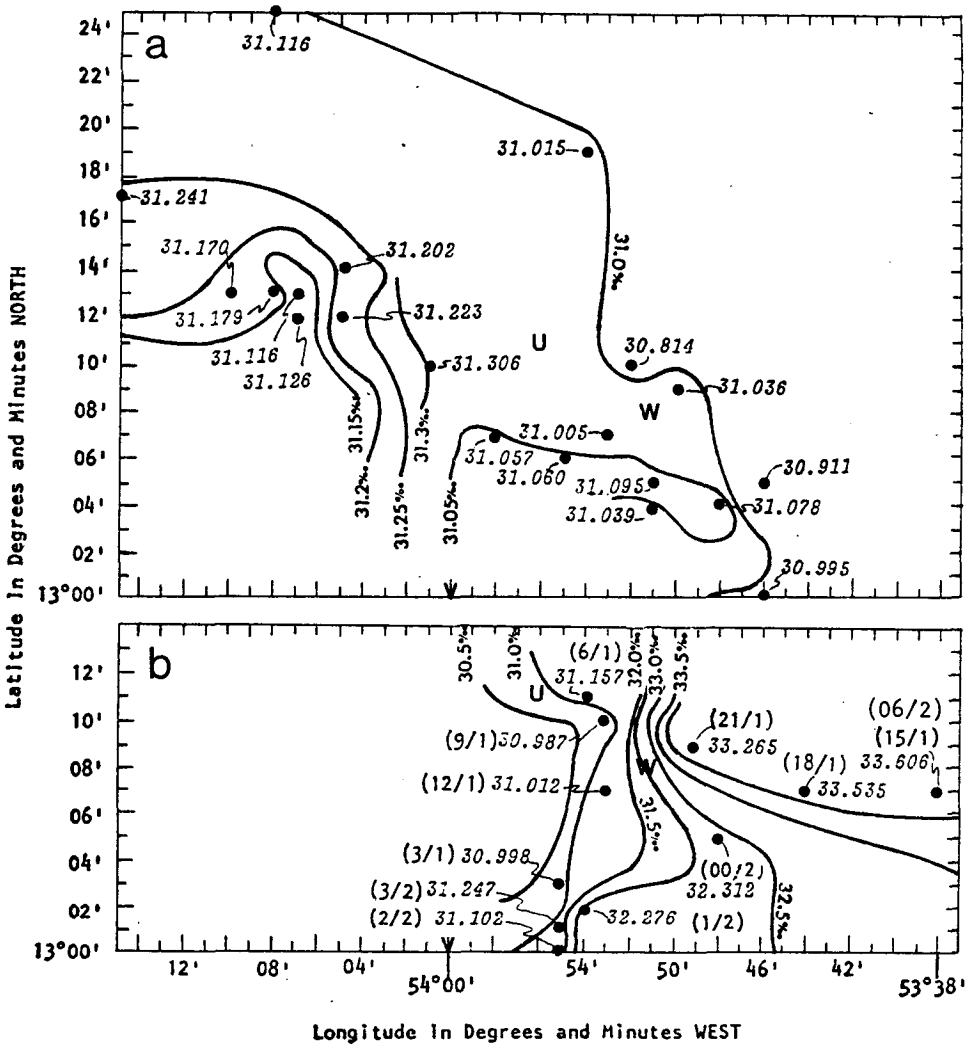

FIG. 5. Horizontal distribution of salinity at −6 m as observed from the *Discoverer* from (a) 2100 GMT 26 June to 0100 GMT 1 July and (b) 0300 GMT 1 July to 0300 GMT 2 July. Salinity distribution is plotted and indicated in parts per thousand (‰) next to each isopleth. Salinity of each point is indicated in italics. Part (b) shows GMT time/day in parentheses next to each salinity value. These maps were constructed by plotting observed salinity while the *Discoverer* was in a drift-stream mode. Stations U, V and W are indicated.

A temperature inversion is evident during approximately the first half of the 12-day period, *viz.*, 22 June–27 June, designated period A. This can be clearly seen in Fig. 6a which shows the time-averaged vertical profile at the regularly scheduled observation times. Despite this temperature inversion the ocean displays static stability because of the presence of low-salinity water in the upper layers (0–15 m) of the ocean (see Fig. 3 and the σ curve on Fig. 6a). Near-surface warming is apparent during most of the 12-day period (see Fig. 2). This eliminates the temperature inversion during the later period B [28 June–2 July (see Fig. 6b); and note the different temperature scales]. The subsurface temperatures at −30 to −35 m do not change very much between the two sets of profiles.

The mean diurnal temperature variation at the surface and at six depths during periods A and B is shown in Figs. 7a and 7b. The diurnal range is indicated on the right-hand side of each curve. At the surface the range observed by the boom sensor is in parentheses. There is good agreement between instruments and periods in the time of occurrence of the maximum temperature departure, *viz.*, 1500 local time (LT). A curious feature of the surface diurnal temperature variation which is seen in the averaged data from Period A is the slight rise in the bucket temperature at 0100 LT. This characteristic also occurs in the surface ob-

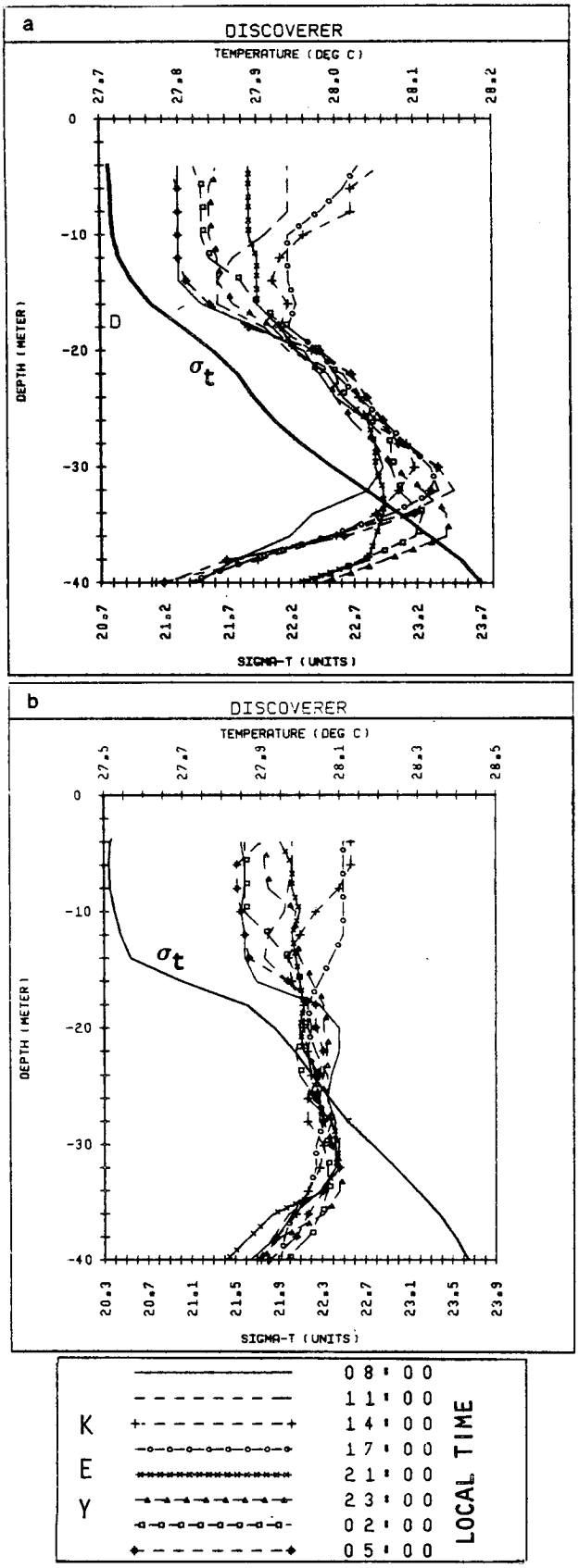

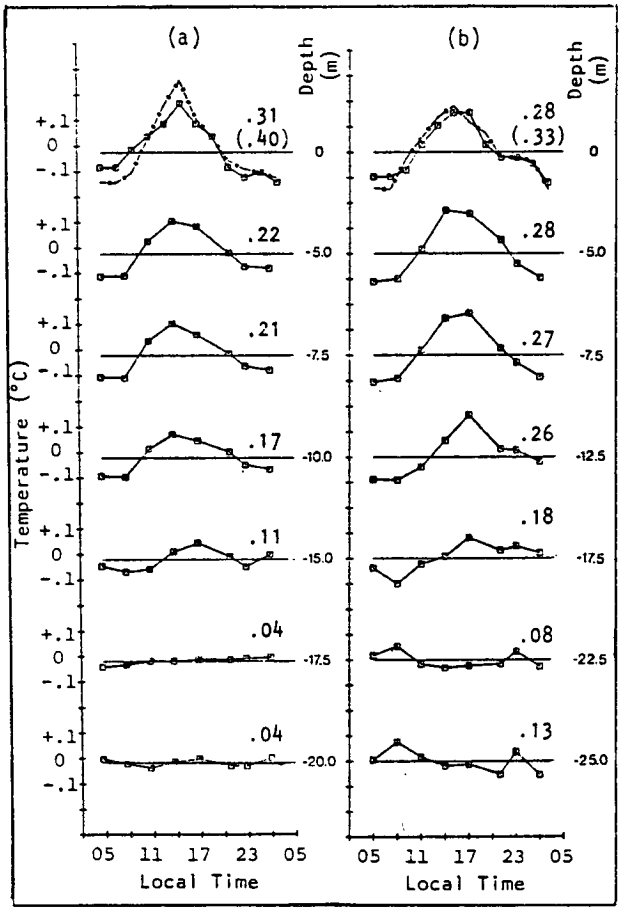

FIG. 7. Mean diurnal temperature variation observed at *Discoverer* during period A (a) and period B (b). The two curves for the surface level represent bucket (□) and boom (○) observations. Temperature variations at subsurface levels are all obtained from STD soundings.

servations at the other two ships, as will be seen later. Its consistency in time and space leads one to believe that it represents a real physical process rather than an idiosyncrasy of the data. It is speculated that it is an effect of continual radiational cooling at the sea surface in the presence of winds which are lighter than those of the daylight hours; a negative temperature gradient (z positive upward) develops, but for some reason overturning does not occur immediately in the early night hours. After some delay the inversion becomes strong enough to allow overturning which brings warmer water up from below. At two of the ships where subsurface temperature inversions persist (*Discoverer* and *Mt. Mitchell*), this secondary

FIG. 6. Diurnal temperature profiles and mean sigma-*t* profiles for the *Discoverer* for (a) 22 June–27 June [period A] and (b) 28 June–2 July [period B]. Depth of penetration of mean diurnal temperature variation is indicated by *D*.

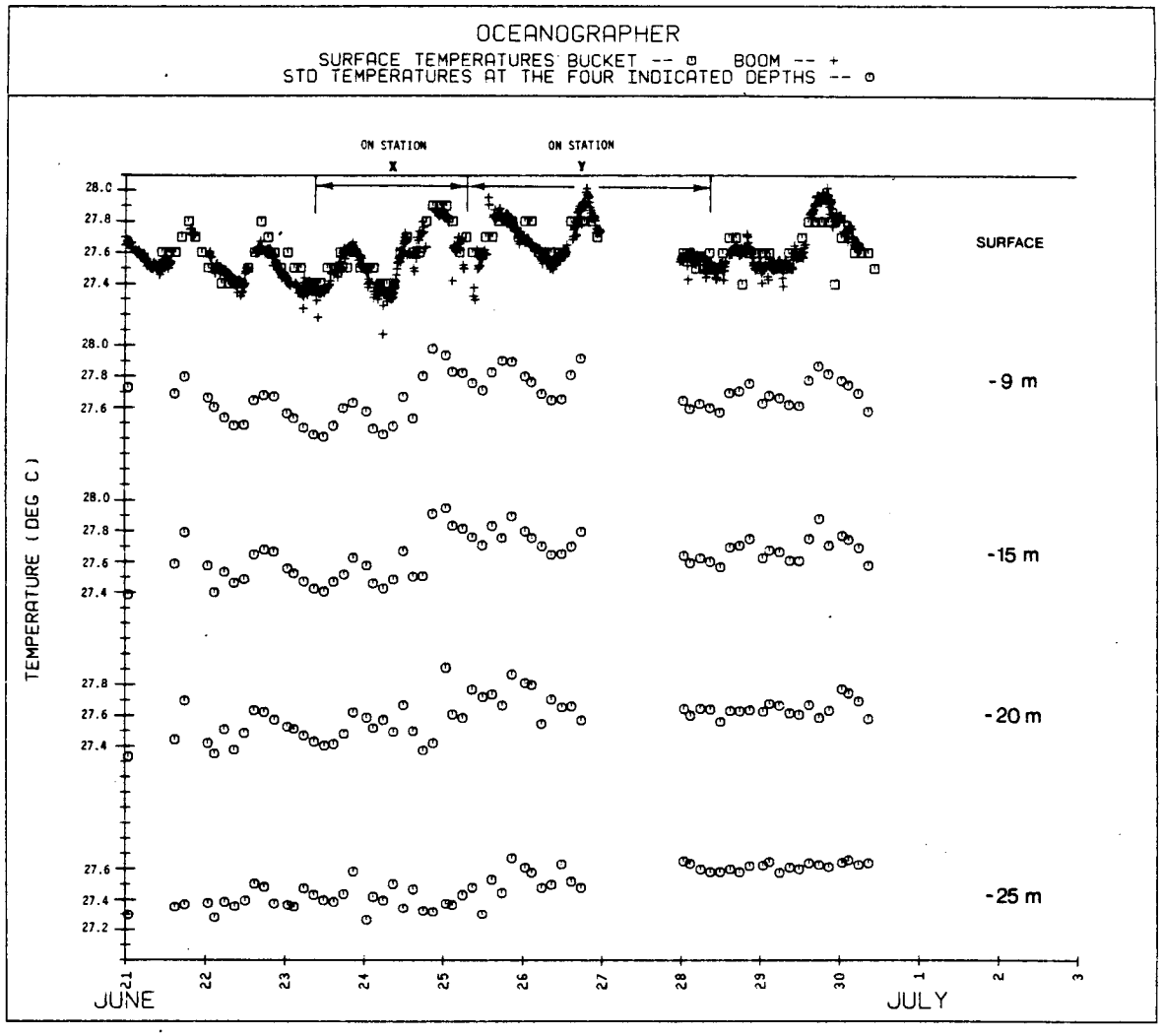

FIG. 8. Water temperatures at *Oceanographer* at sea surface and four subsurface depths as a function of time during Period III. Temperature measurements were made by bucket and boom sensors at surface and by STD soundings at subsurface levels (see box above the figure for symbol designation). At top of temperature axis, the periods for which the ship was on-station are indicated.

temperature maximum could simply result from a gradual deepening of the nocturnal mixed layer.

The mean diurnal range at the surface is larger during Period A than during period B, but at the subsurface levels Period B displays the larger mean amplitudes. The difference in the mean diurnal ranges between periods A and B may be related to the differences in the mean vertical density gradients between the two periods. In the layer between −5 and −14 m the vertical density gradient is about twice as large in period A as it is in period B. This would indicate that the uppermost layers of the ocean were more stable during periods A than B, assuming approximately the same vertical shear of the current. Numerical experiments with alternative forms of the vertical oceanic eddy exchange coefficients have shown that the best diurnal temperature predictions within the mixed layer are made by the coefficients which are functions of the vertical stability (Jacobs, 1978).

The mean diurnal ranges of temperature shown in Fig. 7 are consistent with previously reported values (Defant, 1932; Stommel and Woodcock, 1951; Shonting, 1964; Voskanyan *et al.*, 1967; Howe and Tait, 1969). However, the depth of penetration is less than that reported in all but one of these references. Defant (1932) reported a detectable diurnal temperature variation down to −50 m, but the majority of measurements reported showed no diurnal variation below −30 m. Voskanyan *et al.* (1967) showed measurements in the Black Sea which indicated no variations below −10 m.

b. Observations at the Oceanographer

The *Oceanographer* was able to maintain its position at two stations for several day periods (Delnore and McHugh, 1972). The two stations are designated by X and Y.

The surface and subsurface temperature, as functions of time, are shown at the surface and at the −9, −15, −20 and −25 m levels in Fig. 8. Fig. 9 shows the subsurface salinities at the same levels. The periods in which the ship maintained its position are indicated in both Figs. 8 and 9.

Temperatures measured in the near-surface layer at the *Oceanographer* are cooler than those at the *Discoverer*, with the diurnal variation apparent down to −15 m and occasionally down to −20 m, depending on the amplitude at the surface (see Fig. 8). There is a slight downward trend in the temperatures in the layer between the surface and −9 m during the first 3½ days. A small sudden warming is seen to occur in the −9 to −20 m layer at about the end of the period (when station X was occupied). A warming rise is also seen at −25 m, but occurs more gradually. These elevated temperatures persist throughout the remainder of the observation period. Since the ship was on-station during the time of this temperature change, it is probable that the temperature displays are the result of the passage of a weak thermal front.

The salinity time series also shows trends at all the depths illustrated during both on-station periods. The trend is toward decreasing salinity at −9, −15 and −20 m and toward increasing salinity at −25 m. Near the end of the first on-station period, the trend at each of these depths reverses and persists for the remainder of the data-collection period.

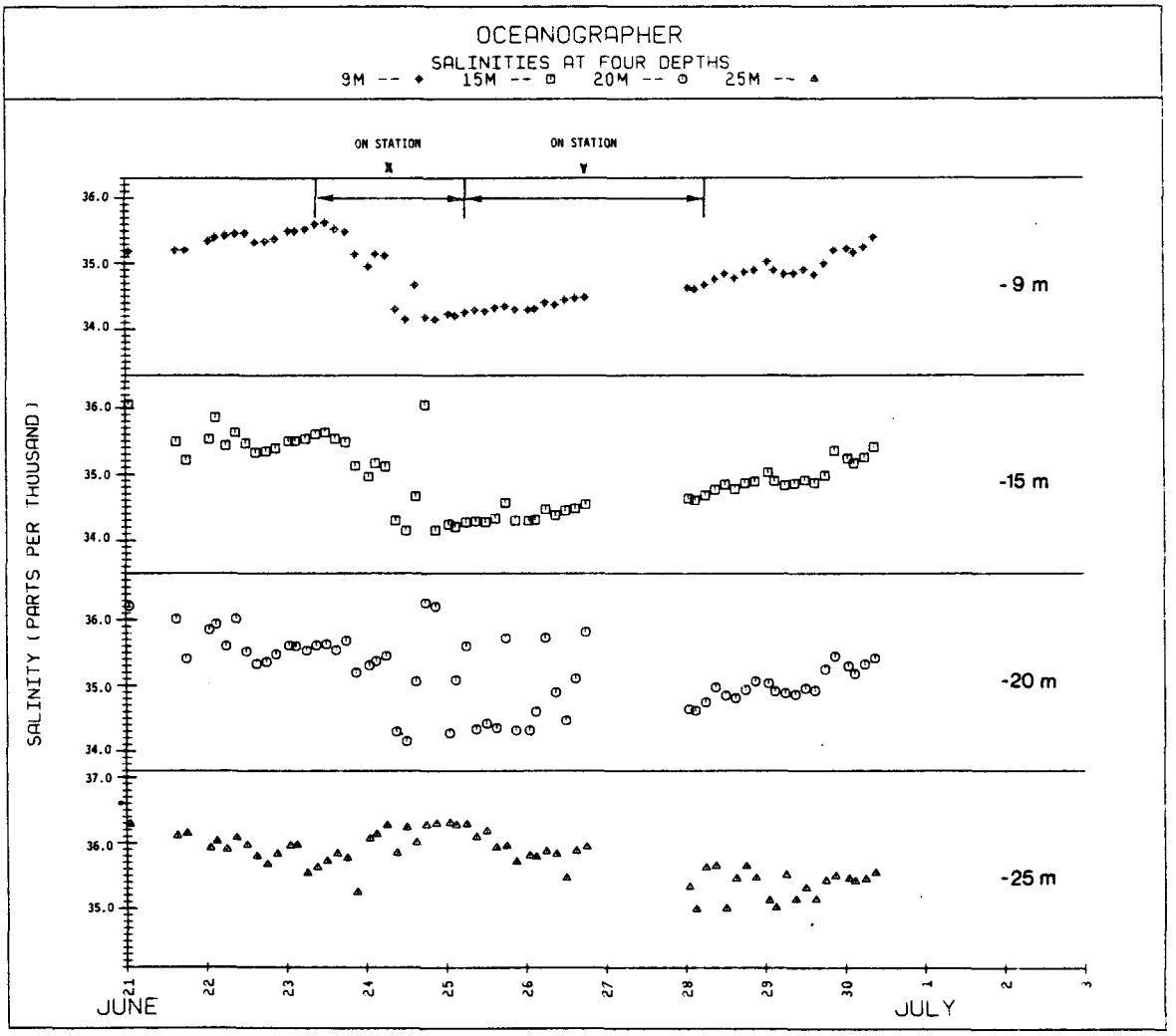

FIG. 9. Salinity at *Oceanographer* at four subsurface depths, as a function of time during Period III (see box above figure for symbol designation). At top of salinity axis, the periods for which the ship was on-station are indicated.

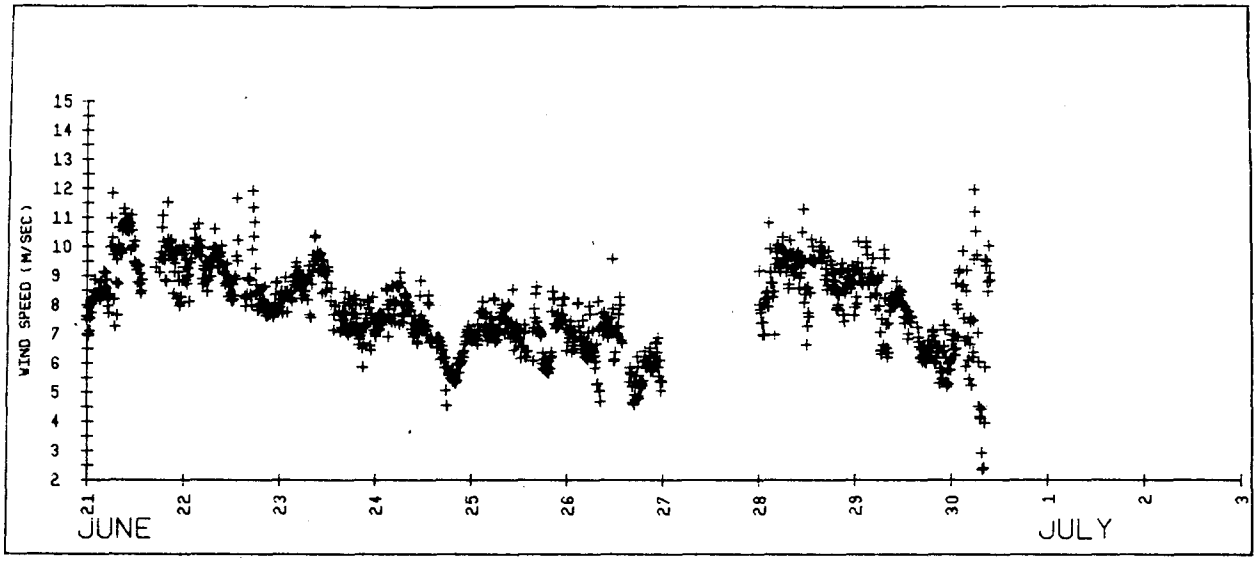

FIG. 10. *Oceanographer* boom observations of wind speed at 10 m above sea surface during Period III. Each point represents a 10 min average of wind speed. The time series was terminated on 30 June because the ship was forced to return to port.

The reversal of the trends occurs during an interval which closely corresponds to the passage of the thermal front. The large scatter in the −20 m salinities (Fig. 9) during the period from 24–26 June is most likely due to internal waves. The internal wave effects are pronounced during this period because advection has enhanced the vertical salinity gradient between the −20 and −25 m levels.

Several events which occur in the temperature and salinity time series can be closely correlated to events in the wind speed which is shown in Fig. 10. The gradual decline in the wind speed begins at about the same time as the downward trend begins in the near-surface salinity. Furthermore, the small dip in the wind speed near the end of the day of 24 June corresponds to the passage of the ocean thermal front, with the minimum occurring at the time of the maximum −9 m temperature. Finally, of the entire 12-day period, 29 June has the largest amplitude diurnal variation in water temperature corresponding to a relatively low wind speed.

In Fig. 11, a pronounced mixed layer is visible in the diurnal temperature profile. However, the mixed layer is considerably deeper in period B than it is in period A. Not only is the mean vertical temperature structure substantially different in these two periods, but it also differs considerably from that observed at the *Discoverer* (see Figs. 6 and 11). The shallowest depth presented in the *Oceanographer* profiles is −6 m because there were insufficient data to construct realistic mean temperature profiles above that depth.

The mean diurnal temperature range at several depths is shown for periods A and B in Figs. 12a and b.

At the surface both boom and bucket measurements show diurnal ranges of about 0.3°C with somewhat greater discrepancies between the methods than those recorded at the *Discoverer*. The time of occurrence of the maximum temperature departure at the surface varies with the method and the period. The averaged boom data for period A reveals a broad maximum between 1100 and 1300 (LST), whereas the bucket data shows a maximum at 1700 LST. In period B, the bucket temperatures show an early maximum at 1100 and the boom a late maximum at 1700. None of the four times of maximum temperature departure at the surface seen in Fig. 12 agrees with the time reported at the *Discoverer*—*viz.*, 1500 LST (see Fig. 7). The *Oceanographer* records also display a secondary maximum at the surface in the early morning hours. The maximum is seen at the boom sensor in both periods.

The depths indicated in Fig. 12a are not the same as those shown in 12b. The data at the −5.0 m level during period B were not sufficient to construct the temperature departure curve. There are also some data problems at this level during period A. These result in a lower than expected temperature departure at 1700 LST since only one observation was obtained in all of Period A at that time and depth. This measurement was made early in the period when temperatures were lower than at the end of the period (see Fig. 8) and therefore the −5 m value from this sounding is unrepresentative of the average temperature departure for that time of the day and that depth.

Despite the inconsistency in the upper two levels shown in the two parts of Fig. 12, it is apparent

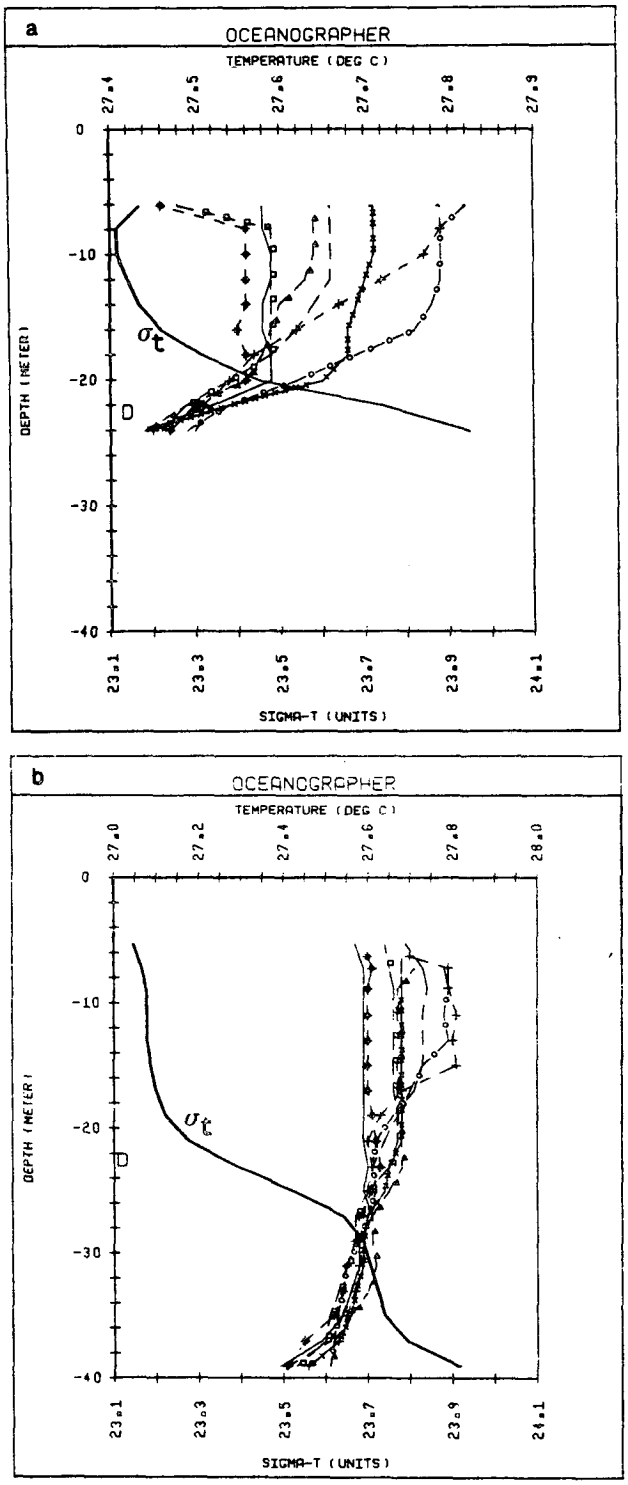

FIG. 11. As in Fig. 6 except for the *Oceanographer*. Note differences in temperature scales for the two parts of the figure.

that there is good agreement between the two periods in the amplitudes of the mean diurnal temperature variation down to a depth of −17.5 m. However, with the vertical resolution shown in Fig. 12 the diurnal heat wave appears to penetrate to −25 m in period B and possibly to −22.5 m in period A. The difference in the depth of penetration is apparently the result of distinctly different vertical thermal structures during these periods (see Fig. 11). The averaged temperature data at −22.5 and −25 m during period A is "noisy", possibly due to the effects of internal waves.

A phase shift with depth is apparent in the time of occurrence of the maximum temperature departure. There is an apparent relationship between the vertical density gradient and the phase shift—*viz.*, the larger the vertical density gradient between the depths, the larger the shift. This observed behavior suggests that if the vertical turbulent processes are parameterized, the best results would be obtained from a form of parameterization that is a function of the vertical stability. The results of Jacobs (1978) support this suggestion.

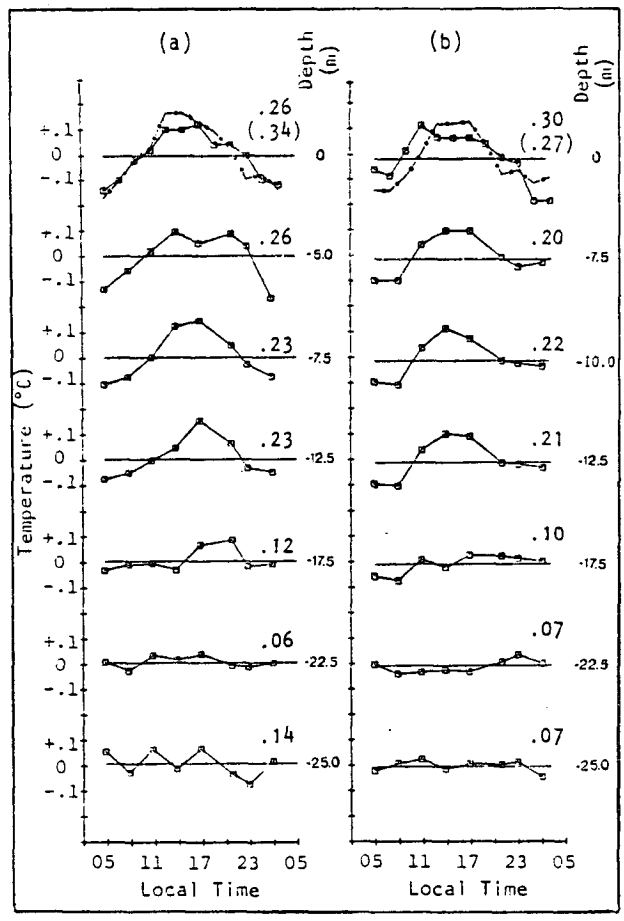

FIG. 12. Mean diurnal temperature variations observed at *Oceanographer* during period A (a) and period B (b). The two curves for the surface level represent bucket (□) and boom (○) observations. Temperature variations at subsurface levels are all obtained from STD soundings.

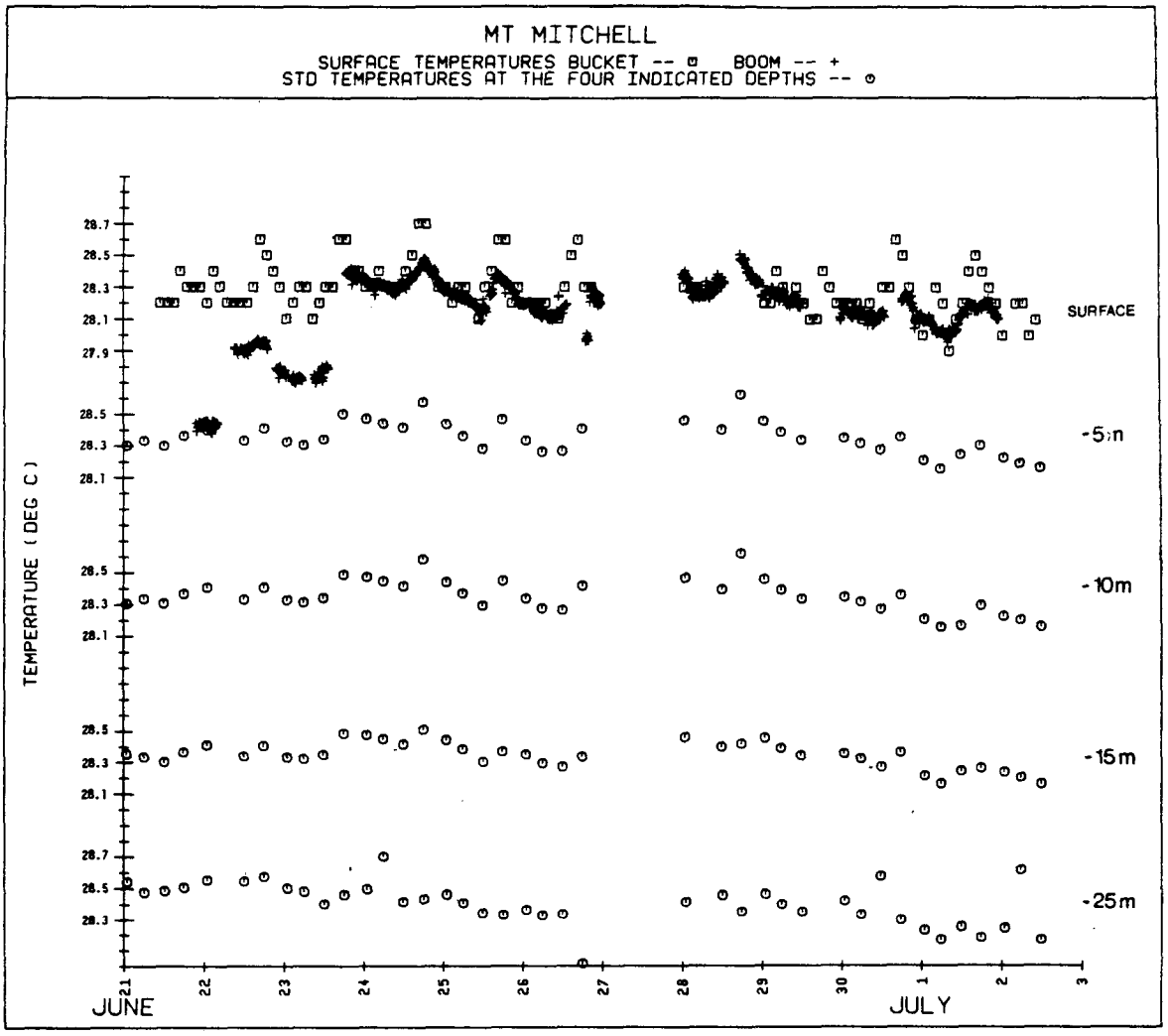

FIG. 13. Water temperature at *Mt. Mitchell* at sea surface and four subsurface depths as a function of time during Period III. Temperature measurements were made by bucket and boom sensors at surface and STD sounding at subsurface levels (see box above the figure for symbol designation).

c. *Observations at the Mt. Mitchell*

Of the three ships, the *Mt. Mitchell* was able to maintain its position within the smallest area during Period III. The ship remained within such close proximity to its mean position that it could be considered as on-station during the entire 12-day period. The surface and subsurface temperatures are displayed as time series in Fig. 13, and the subsurface salinities are presented in Fig. 14. The levels below the surface, shown in Figs. 13 and 14, are −5, −10, −15 and −25 m.

The reported boom observations of the sea surface temperature during the first two days of the period simulated contain obvious systematic errors. Also, the midday boom observations differ significantly from the midday bucket observations for the remainder of the measurement period. From 21 June through 23 June, the amplitude of the diurnal heating is noticeably diminished with depth down to −15 m. During this period, a large increase in salinity takes place at all depths shown in Fig. 14. In the remainder of the observation period, an inverse correlation between temperature and salinity exists. That is, from 28 June through midday 2 July slight increases in temperature are accompanied by slight decreases in salinity and vice versa.

There also appears to be a relationship at the *Mt. Mitchell* between temperature and salinity fluctuations, and those of wind speed. The 10 m wind speed is shown in Fig. 15. The major salinity front with its associated weak temperature front appears to have completed its passage by the ship early on 24 June. Starting at about

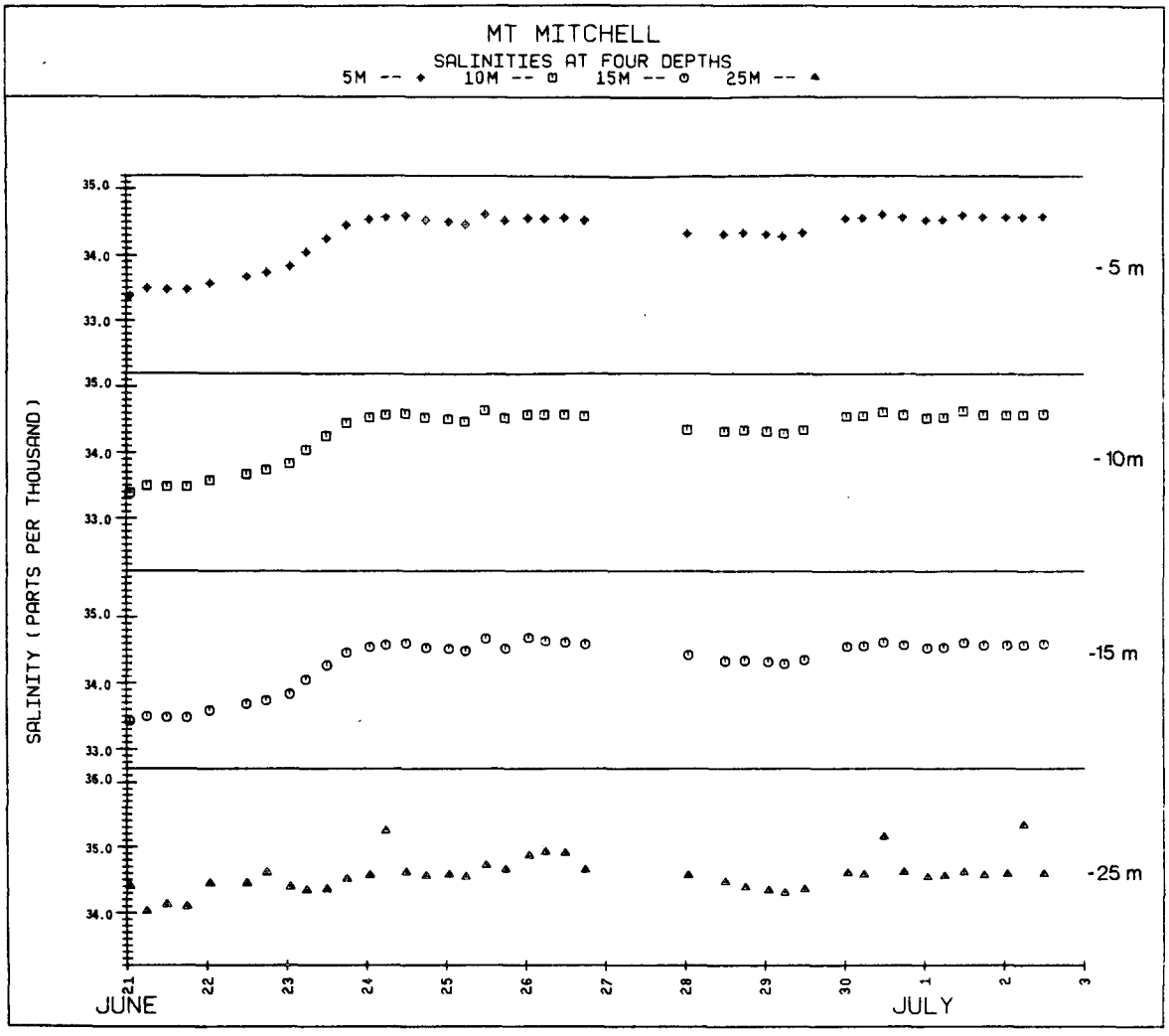

FIG. 14. Salinity at *Mt. Mitchell* at four subsurface depths as a function of time during Period III (see box above figure for symbol designation).

this time, the wind speed decreased slightly through 27 June.

The vertical profiles of the averaged temperature at a fixed time of day are shown in Fig. 16 for the two halves of the 12-day observing period. A temperature inversion centered at about −40 m persists throughout this entire period and is actually intensified during its second half (Fig. 14b) by decreasing near-surface temperatures (see Fig. 13).

Since STD casts at the *Mt. Mitchell* were taken every 6 h, the mean diurnal temperature variation as a function of depth shown for the two halves of Period III in Fig. 17 is more coarsely defined than at the other ships. Nevertheless, the diurnal variation is clearly evident down to −17.5 m.

The surface temperature departures for the bucket and boom observations are significantly different in amplitude during periods A and B and different in phase during period A. The amplitude of the bucket surface temperatures for period A is the largest of any seen at the three ships; that of the boom temperature during period B is the smallest. Maximum temperature departures occur at 1300 and 1500 LST in the bucket temperatures during periods A and B, respectively. The earlier time corresponds to that of the maximum in boom temperature at the *Oceanographer* and the later to that of the *Discoverer*. Secondary maxima in the surface temperatures at 0100, which are seen at the other ships, are clearly evident in the bucket temperatures. In both periods, this phenomenon is even more apparent during the first few days of the surface bucket temperature time series (see Fig. 13, 22–25 June). The mean boom temperature variations during period A have apparently been contaminated by instrument calibration error during the first two days of the averaging period

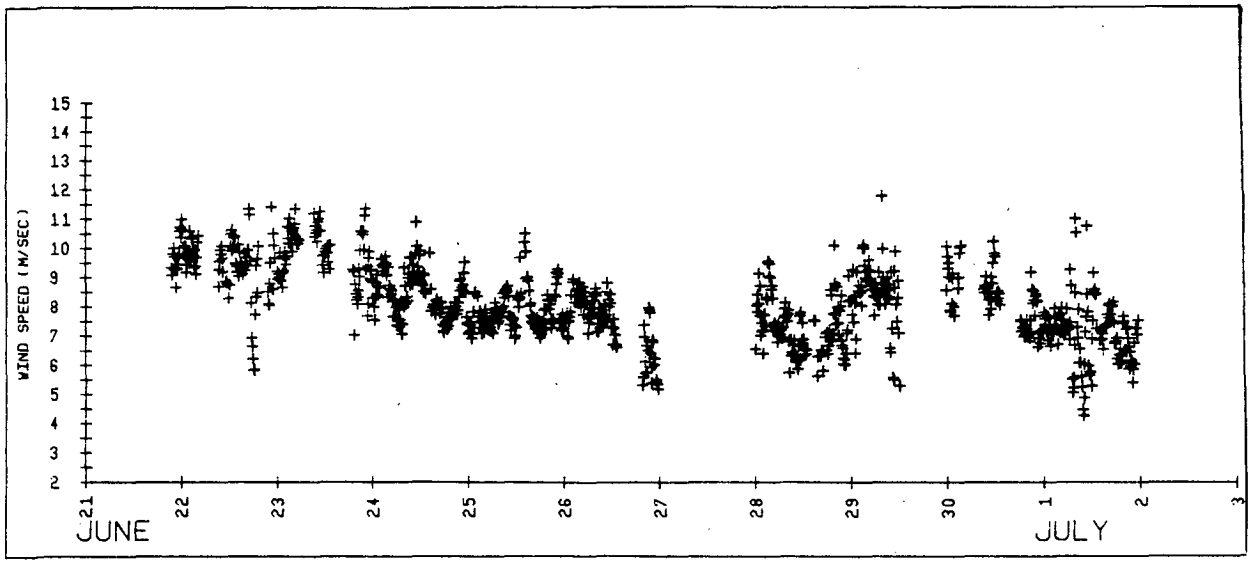

FIG. 15. *Mt. Mitchell* boom observations of wind speed at 10 m above sea surface during Period III. Each point represents a 10 min average of the wind speed.

(see Fig. 13). Despite this, the average boom observations for period A reveal a better defined diurnal temperature variation than the observations collected during period B. The maximum values occur at 1700 and 1500 for the respective periods. The later time corresponds to that seen in the *Oceanographer* bucket temperatures and the earlier time agrees with that seen at the *Discoverer*.

The amplitude of subsurface temperature variation is less than that seen at the other ships. This probably results from the coarse time resolution which did not allow the true range of temperature variation to be recorded. The temperature departures at the −22.5 and −25 m levels in periods A and B appear to have a diurnal period, but the amplitudes of the temperature variation are larger than at the −17.5 m level. This suggests that there are other physical processes influencing the temperatures at that depth, *viz.*, tidally induced internal waves. Subsurface maximum temperature departures down to −12.5 m occur at 1400 LST. This can be considered to be in phase with the bucket observations since the scheduled observation times for the bucket and STD casts differ by 1 h at that time of day. The maximum temperature departure in both periods at −17.5 m occurs 6 h later than at −12.5 m. The coarse time resolution makes it difficult to define the actual phase shift with respect to depth. However, there is no apparent phase shift in the maximum temperature departures seen in Fig. 17a (period A) between −17.5 and −22.5 m and a 5 h phase shift within the same layer for period B. Within the layer the mean vertical density gradient is considerably larger in period A than in period B (see Fig. 16). This again suggests a relationship between the effective vertical turbulent transfer of heat and the vertical density gradient.

3. Summary

Several sets of near-surface air and water observations collected during Period III of BOMEX are presented. The natural variability displayed in these observations is examined and several interesting features are noted. These features are as follows:

- The overall variability in time and space of the observed salinity is larger than might have been expected in the trade wind regime. These variations are most likely the effects of advection and internal waves, but definite confirmation is difficult with the limitations of the BOMEX oceanographic data set.
- There is a possible correlation between the 10 m wind speed and the movement of small-scale oceanic salinity and temperature fronts which deserves further study.
- A secondary nocturnal maximum in the mean diurnal variation of the sea-surface temperature appears at all three ships.
- The mean diurnal temperature range is small compared to those reported previously and demonstrates considerable variability in time (periods A and B) and space (both horizontal and vertical).

In addition, the relation between the amplitude,

phase shift with depth, and depth of penetration of the mean diurnal temperature variation within the upper layers of the ocean and the vertical density gradients is suggested. This relationship

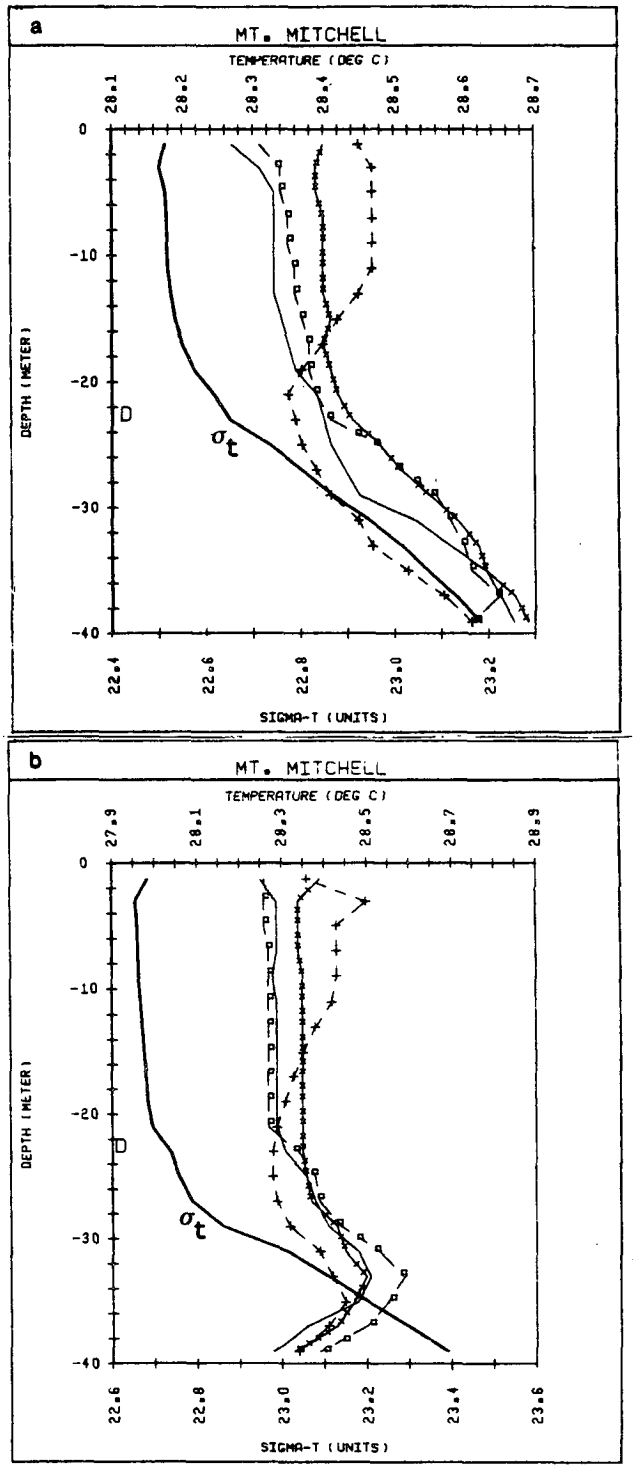

FIG. 16. As in Fig. 6 except for the *Mt. Mitchell*. Note difference in temperature scale between the two parts of the figure.

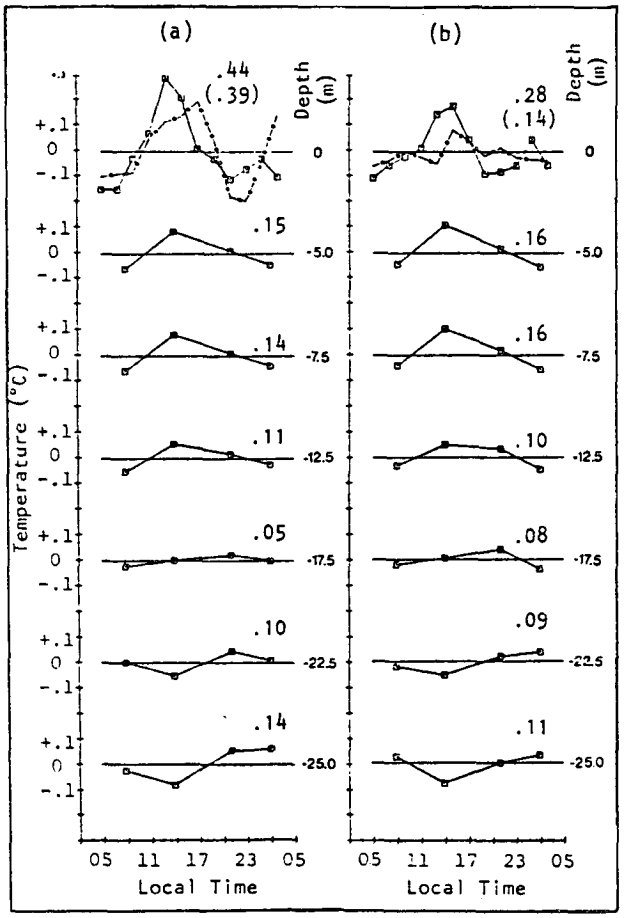

FIG. 17. Mean diurnal temperature variations observed at *Mt. Mitchell* during period A. The two curves for the surface level represent bucket (□) and boom (○) observations. Temperature variations at subsurface levels are all obtained from STD soundings.

is consistent with recent numerical model experiments (Jacobs, 1976, 1978).

Acknowledgments. This paper is based on material included in the author's Ph.D. thesis. The guidance and supervision of Prof. Gerhard Neumann of the Department of Earth and Planetary Sciences at City University of New York and Dr. Joseph Pandolfo, Dr. Jerome Spar and Prof. James Miller are much appreciated.

Thanks are extended for their excellent work to Ms. Mary-Ellen Albert for preparing the manuscript, and to Ms. Diane Blackman for assisting in the preparation of material for the manuscript.

I am grateful to Mr. V. E. Delnore for his discussions concerning BOMEX, in which he participated, and his loan of some art work used in this manuscript.

Research was supported by the Atmospheric Sciences Section of the National Science Foundation under Grant GA-27942.

REFERENCES

BOMAP, 1971: BOMEX field observations and basic data inventory. Barbados Oceanographic and Meteorological Analysis Project Office, NOAA, Rockville, Md., 428 pp.

Defant, A., 1932: Die Gezeiten und inneren Gezeitenwellen des Atlantischen Ozeans. *Wiss. Erg. Dtsch. Atlantische Expedition "Meteor"* 1427–1927, Vol. 7, No. 1, Berlin, Walter de Gruyter, 318 pp.

Delnore, V. E., 1972: Diurnal variation of temperature and energy budget for the oceanic mixed layer during BOMEX. *J. Phys. Oceanogr.*, **2**, 239–247.

Delnore, V. E., and J. McHugh, 1972: BOMEX Period III upper ocean soundings. NOAA, Rockville, Md.; 352 pp.

Holland, J., 1972: Comparative evaluation of some BOMEX measurements of sea-surface evaporation, energy flux and stress. *J. Phys. Oceanogr.*, **2**, 476–486.

Howe, M. R., and R. I. Tait, 1969: Some observations of the diurnal heat wave in the ocean. *Limnol. Oceanogr.*, **14**, 16–22.

Jacobs, C. A., 1976: Numerical experiments with alternative formulations of oceanic vertical eddy exchange coefficients using BOMEX data. Ph.D. dissertation, New York University, 169 pp.

——, 1978: Numerical simulations of the natural variability in water temperature during BOMEX using alternative forms of the vertical eddy exchange coefficients. *J. Phys. Oceanogr*, **8**, 119–141.

Landis, R. C., 1971: Early BOMEX results of sea surface salinity and Amazon River water. *J. Phys. Oceanogr.*, **1**, 278–281.

MacIntyre, F., 1974: The top millimeter of the ocean. *Sci. Amer.*, **230**, 62–77.

Metcalf, W. G., 1968: Shallow currents along the northeastern coast of South America. *J. Mar. Res.*, **26**, 232–243.

Neumann, G., 1969: Seasonal salinity variations in the upper strata of the western tropical Atlantic Ocean—I. Sea surface salinities. *Deep-Sea Res.*, **16**, 165–177.

Pandolfo, J. P., and C. A. Jacobs, 1972: Numerical simulations of the tropical air-sea planetary boundary layer. *Bound.-Layer Meteor.*, **3**, 15–46.

Pond, S., G. T. Phelps, J. E. Paquin, G. McBean and R. W. Stewart, 1971: Measurements of the turbulent fluxes of momentum, moisture, and sensible heat over the ocean. *J. Atmos. Sci.*, **28**, 901–917.

Ryther, J. H., D. W. Menzel, and N. Corwin, 1967: Influence of Amazon River outflow on the ecology of the western tropical Atlantic, I. Hydrography and nutrient chemistry. *J. Mar. Res.*, **25**, 69–83.

Shonting, D. H., 1964: Some observations of the short-term heat transfer through the surface layers of the ocean. *Limnol. Oceanogr.*, **9**, 576–588.

Stommel, H., and A. Woodcock, 1951: Diurnal heating of the surface of the Gulf of Mexico in the spring, 1942. *Trans. Amer. Geophys. Union*, **32**, 563–571.

Voskanyan, A. G., A. A. Pivovarov and G. G. Khundzhua, 1967: The diurnal temperature variation and turbulent exchange with heating of the sea surface layer. *Bull. Acad. Sci. USSR Atmos. Oceanogr. Phys.*, **3**, 711–714.